www.nature.com/aps

Acta Pharmacologica Sinica

ARTICLE

Transcription factor Klf9 controls bile acid reabsorption and enterohepatic circulation in mice via promoting intestinal Asbt expression

Shuang Liu[1], Man Liu[1], Meng-lin Zhang[1], Cui-zhe Wang[2], Yin-liang Zhang[1], Yu-jie Zhang[1], Chun-yuan Du[1], Su-fang Sheng[1], Wei Wang[3], Ya-tong Fan[1], Jia-ni Song[1], Jin-can Huang[1], Yue-yao Feng[1], Wei Qiao[1], Jin-long Huang[1], Yu-hui Li[1], Lu Zhou[4], Jun Zhang[2] and Yong-sheng Chang[1]

Bile acid (BA) homeostasis is regulated by the extensive cross-talk between liver and intestine. Many bile-acid-activated signaling pathways have become attractive therapeutic targets for the treatment of metabolic disorders. In this study we investigated the regulatory mechanisms of BA in the intestine. We showed that the BA levels in the gallbladder and faeces were significantly increased, whereas serum BA levels decreased in systemic Krüppel-like factor 9 (Klf9) deficiency ($Klf9^{-/-}$) mice. These phenotypes were also observed in the intestine-specific Klf9-deleted ($Klf9^{vil-/-}$) mice. In contrast, BA levels in the gallbladder and faeces were reduced, whereas BA levels in the serum were increased in intestinal Klf9 transgenic ($Klf9^{Rosa26+/+}$) mice. By using a combination of biochemical, molecular and functional assays, we revealed that Klf9 promoted the expression of apical sodium-dependent bile acid transporter (Asbt) in the terminal ileum to enhance BA absorption in the intestine. Reabsorbed BA affected liver BA synthetic enzymes by regulating Fgf15 expression. This study has identified a previously neglected transcriptional pathway that regulates BA homeostasis.

Keywords: Klf9; Asbt; bile acid; Fgf15

Acta Pharmacologica Sinica (2022) 43:2362–2372; https://doi.org/10.1038/s41401-021-00850-x

INTRODUCTION

Bile acids are amphipathic steroid molecules synthesized from cholesterol in the liver and secreted into the intestine via the biliary system. BAs are efficiently reabsorbed in the ileum and taken up by hepatocytes from the portal blood [1, 2]. BAs play multiple roles in carbohydrate and lipid metabolism [3, 4]. Numerous enzymes and transporters in enterohepatic circulation are essential to maintain the size and composition of the BA pool. Impaired regulation of BA excretion leads to the occurrence of metabolic disorders, which are associated with hypercholesterolemia, BA malabsorption and type 2 diabetes [5, 6].

Two pathways regulate BA synthesis in hepatocytes: cytochrome P450 family 7 subfamily A member 1 (Cyp7a1) is a classic pathway that limits the *de novo* synthesis of BAs, whereas cytochrome P450 family 27 subfamily A member 1 (Cyp27a1) is an important enzyme in the alternative pathway [7]. The hepatocellular transport of BAs is critical in enterohepatic circulation. Na^+-taurocholate cotransporting polypeptide (Ntcp) and the organic anion transporting polypeptide (Oatp) family are responsible for transporting BAs efficiently from the portal blood into hepatocytes [8]. Organic solute transporters α/β (Ostα/β) located in the basolateral membrane transport BAs into portal circulation [9]. BAs are shuttled across hepatocytes to the canalicular membrane by bile salt export pump (Bsep) and Mdr2/3 for secretion into bile [10]. Enzymes and transporters are regulated by farnesoid X receptor (Fxr), small heterodimer partner (Shp) and fibroblast growth factor (Fgf) 15 [11, 12].

More than 95% of BAs passing through the small intestine are reabsorbed at the distal ileum. The apical sodium-dependent bile acid transporters (SLC10A2, Asbt) and Ostα/β are able to transport BAs [13, 14]. Asbt is the main transporter for BA reabsorption in the small intestine. The loss of faecal BAs in Asbt-knockout (KO) mice is 10–20 times higher than that in wild-type (WT) mice. Although liver BA synthesis is increased via feedback from enterohepatic circulation, the BA pool in Asbt-KO mice was substantially lower than that in WT mice [15]. Asbt inhibition resulted in BAs composition changes and improved glucose tolerance and steatohepatitis pathology in high-fat diet-fed mice [16]. Previous studies demonstrated that BAs in the intestine bind to Fxr to induce the endocrine hormone Fgf-15 (Fgf19 in humans), which in turn activates hepatic receptors through the portal vein to inhibit BA synthesis [5, 15–17]. Moreover, Fgf15 activation

[1]Key Laboratory of Immune Microenvironment and Disease (Ministry of Education), Tianjin Key Laboratory of Cellular Homeostasis and Disease, Department of Physiology and Pathophysiology, Tianjin Medical University, Tianjin 300052, China; [2]Department of Basic Medicine, Shihezi University School of Medicine, Shihezi 832000, China; [3]Key Laboratory of Biotechnology of Hubei Province, Key Laboratory of Biotechnology of Chinese Traditional Medicine, National & Local Joint Engineering Research Center of High-throughput Drug Screening Technology, Hubei University, Wuhan 430062, China and [4]Department of Gastroenterology and Hepatology, Tianjin Medical University General Hospital, Tianjin 300052, China

Correspondence: Lu Zhou (lzhou01@tmu.edu.cn) or Jun Zhang (zhangjunyc@163.com) or Yong-sheng Chang (changys@tmu.edu.cn)

These authors contributed equally: Shuang Liu, Man Liu

Received: 10 September 2021 Accepted: 21 December 2021
Published online: 1 February 2022

induces Fxr phosphorylation at Y67 for the feedback regulation of BAs [18].

Krüppel-like factor 9 (Klf9) belongs to a family of transcription factors that contain GC box-binding proteins [19]. Klf9 regulates a variety of biological functions, such as haematopoietic dysfunction, thermogenesis of brown and beige fat [20], and the migration and invasion of cancer cells [21–23]. Previous experiments showed that Klf9 reduces crypt stem/transit cell proliferation, and Klf9-null mutant mice have shorter villi [24]. However, the function of Klf9 in intestinal BA metabolism is unknown.

In this study, we identified the physiological function of Klf9 in the intestine and found that Klf9 promotes Asbt expression and BA reabsorption. In mechanistic studies, we showed that Klf9 directly binds to and activates the Asbt gene promoter in the intestine. The increase in Fgf15 expression in response to the high BA level in the intestine contributes to the decrease in BA synthesis in hepatocytes.

MATERIALS AND METHODS

Animal studies

Global Klf9 mutant (Klf9($^{-/-}$)) mice were obtained from the Jackson Laboratory (No. 012909). Klf9 transgenic mice (Klf9^{rosa26}) were generated at Beijing Biocytogen Co., Ltd. The generation of systemic Klf9$^{flox/flox}$ mice by the CRISPR/Cas9 system was previously described [25]. Albumin-Cre mice were a gift from Hongbing Zhang (Peking Union Medical College). Villin-Cre mice were purchased at Viewsolid Biotech. All mice were backcrossed onto a C57BL/6 background. The mice (male, 8–10 weeks old) were sacrificed after a 12-h light/12-h dark cycle. All animal experiments were approved by the Ethical Committee of Tianjin Medical University General Hospital.

Cell culture

HEK293T and HEK293A cells were cultured in Dulbecco's modified Eagle's medium (DMEM) with 10% foetal bovine serum (FBS) and 1% penicillin/streptomycin. Caco-2 cells were incubated with DMEM with 10% FBS and 1% penicillin/streptomycin and then induced to differentiate and transfected with adenovirus. Primary mouse small intestine epithelial cells were isolated from C57BL/6 mice. The ileum was cut into 1 mm pieces and incubated in a buffer containing 0.05% (*w/v*) collagenase type IV (Millipore Sigma) in a 37 °C water bath for 25 min to allow the isolation of single epithelial cells. The cells were washed three times with ice-cold PBS and centrifuged at 500 × *g* for 5 min. The isolated epithelial cells were suspended in advanced DMEM/F12 (Invitrogen) containing insulin–transferrin sodium selenite, 0.1% hydrocortisone, 5% FBS and 1% *L*-glutamine.

Plasmid constructs

All plasmids used in this study were prepared as previously described [25]. The sequences of the *Klf9* gene were amplified from cDNA obtained by mRNA reverse transcription. The PCR-amplified sequences were inserted into the pAd-Track CMV shuttle vector. Purified lentiviruses for sh-control and shRNA were purchased from Vector Builder. All plasmids were verified through sequencing. The recombinant adenovirus plasmids were transfected into HEK-293A cells for the augmentation of recombinant adenoviruses.

RNA isolation and real-time quantitative polymerase chain reaction (RT-qPCR)

Total RNA was extracted from mouse tissues or cells using TRIzol following the manufacturer's instructions (Invitrogen). Purified RNA (2 μg) was subjected to reverse transcription using the Applied Biosystems high-capacity cDNA reverse-transcription kit. Complementary DNA (cDNA) was analysed by quantitative PCR using SYBR Green PCR Master Mix (Promega) on a Bio-Rad C1000 thermal cycler CFX96 Real-Time System. The relative expression of each mRNA was calculated by the comparative Ct method normalised to that of 36B4. The primer sequences are shown in Supplementary Table 1.

Luciferase reporter assays

The 5′-ends of mouse Fgf15 and Asbt mRNAs were amplified by PCR. The PCR product was subcloned into the pGL3-Basic (Promega) luciferase reporter plasmid with *Mlu*I/*Xho*I (Fgf15) or *Kpn*I/*Xho*I (Asbt) sites. All PCR products were sequenced to confirm the correct directionality of the inserted sequence. HEK-293A cells were seeded in 24-well plates and transfected with 100 μg Klf9-Luc and each of the indicated luciferase promoters or pcDNA3.1 (control). Under all conditions, the cells were cotransfected with 2 μg pRL-CMV *Renilla*-expressing vector (*Renilla* luciferase expression vector) and incubated in serum-free medium for 6 h. Then, the medium was replaced with DMEM containing 10% FBS for another 48 h. Luciferase activity was analysed for luciferase and *Renilla* luminescence using the Dual-Glo® Luciferase Assay System Protocol (Promega, E2940) according to the manufacturer's instructions.

ChIP assay

Briefly, 2×10^7 Caco-2 cells were infected with Klf9-3×Flag or GFP for 48 h. Then, the cells were treated with 1% formaldehyde at room temperature for 10 min and lysed with ChIP cell lysis buffer (10 mM Tris-HCl [pH 8.0], 10 mM NaCl, 3 mM $MgCl_2$, 0.5% NP-40 and protease inhibitor cocktail) and ChIP nuclear lysis buffer (50 mM Tris-HCl [pH 8.0], 5 mM EDTA, 1% sodium dodecyl sulphate [SDS], and protease inhibitor cocktail). Cell lysates were sonicated to shear the chromatin and immunoprecipitated with antibodies specific for Flag (Sigma-Aldrich; catalogue F7425) or unspecific IgG (Santa Cruz Biotechnology Inc.; catalogue sc-2027). The immunoprecipitates were isolated using protein G-agarose beads (Invitrogen) and then washed and eluted with 1% SDS in 0.1 M $NaHCO_3$. We reversed the crosslinks by incubation at 65 °C overnight and used proteinase K digestion. Then, the immunoprecipitated DNA fragments and input DNA were recovered by a PCR purification kit (Qiagen). The purified DNA was used to amplify the Klf9 regulatory element on the mouse Asbt promoters.

Western blot analysis

The liver and ileum were removed from C57BL/6 mice and homogenised in lysis buffer (20 mM Tris-Cl pH 7.5, 140 mM NaCl, 1 mM $CaCl_2$ and $MgCl_2$, 10 mM NaF, 1% NP-40, 10% glycerol, 2 mM Na-vanadate and 1 mM PMSF) containing protease inhibitor cocktail (Roche). The mixture was sonicated and centrifuged at 12,000 × *g* for 20 min at 4 °C. Equal amounts of protein were loaded on a 10% SDS–polyacrylamide gel. Immunoblotting was performed using the following primary antibodies: Klf9 (ABclonal, catalogue A7196), Cyp7a1 (Millipore Sigma, catalogue AB3242), Asbt (Absin, catalogue abs143593), Fgf15 (Santa Cruz Biotechnology, catalogue sc-514647) and β-actin (ABclonal, catalogue AC026). Protein expression was quantified using a Microtek Scan Maker.

Histopathology evaluation

Mouse tissues (liver and ileum) were fixed with 10% neutral formalin and then cut into 4 μm-thick paraffin sections. Dewaxed sections were stained with haematoxylin and eosin for microscope observation (Zeiss).

Immunohistochemistry

Tissue specimens were deparaffinized and then blocked with 5% horse serum for 30 min and incubated with primary antibody (rabbit polyclonal anti-Asbt, 1:100, Abcam) overnight at 4 °C. The tissue sections were washed three times with PBS and incubated with prediluted horseradish peroxidase-conjugated secondary

antibody (1:200) for 2 h. Finally, the slides were stained with diaminobenzidine for colorimetric detection, counterstained with haematoxylin and mounted under coverslips. The immunohistochemistry staining of Asbt was analysed by Image-Pro Plus 6.0 software.

Tissue harvesting and biochemical analysis of BAs

Faeces were dried at 55 °C for 48 h and then extracted with 95% ethanol at 55 °C overnight, 80% ethanol for 2 h and methanol/chloroform (2:1) once for 2 h at 55 °C. The alcoholic extracts were centrifuged, and the supernatants were collected. The serum samples were used directly. A BA assay kit (Jianglaibio, Shanghai, China) was used for the quantitative analysis of BAs.

Immunofluorescence

Intestinal sections were deparaffinized and rehydrated by immersing the slides in different ethanol concentrations. Antigen retrieval was performed in a microwave with 10 mM sodium citrate buffer (pH 6.0). The sections were blocked with 5% BSA for 30 min at room temperature and incubated overnight at 4 °C with the primary antibodies (anti-Fgf15, 1:50 dilution, Santa Cruz). Then, the tissues were washed twice with 1% serum PBS-T for 10 min each, and then incubated with secondary antibodies (Alexa Fluor 488-conjugated anti-mouse IgG, A21202) containing 0.05%–0.1% Triton X 100 for 1–2 h at room temperature. Subsequently, the sections were washed three times with PBS and mounted with DNA binding dye (4′,6-diamidino-2-phenylindole). All images were collected with a confocal microscope (Zeiss LSM 780).

Measurement of TC and TG levels

The TC and TG levels in the plasma and hepatocytes were determined by enzymatic assay according to the manufacturer's recommendation (Applygen Technologies E1013). The absorbance at 570 nm was measured with a microporous plate spectrophotometer (Epoch, America).

ELISA

A mouse FGF15 ELISA kit (catalogue: CSB-EL522052MO) was purchased from CUSABIO (Wuhan, China). The concentration of mouse serum FGF15 was measured following the manufacturer's instructions

Statistical analysis

All data were analysed using SPSS (version 22.0) and are presented as the mean ± standard error of the mean (SEM). Statistical differences between the two individual groups were analysed with Student's *t* test. $P < 0.05$ was considered statistically significant. The minimum number of each set of animals was 5. The results are representative images obtained from experiments that were repeated independently at least three times.

RESULTS

Klf9 deletion results in BA dysregulation

We previously demonstrated that Klf9 regulates hepatic glucose metabolism and energy metabolism of thermogenic fat [20, 26]. Moreover, we observed that gallbladder volume was larger in the global Klf9 KO mice ($Klf9^{-/-}$) than in the WT mice (Fig. 1a). We measured the BA levels in the gallbladder, faeces and serum. The BA levels in the gallbladder and faeces were remarkably increased whereas serum BA levels were decreased in the $Klf9^{-/-}$ mice (Fig. 1b). BAs are critical for lipid absorption. Thus, we assessed the effect of Klf9 deficiency on triglyceride (TG) and cholesterol absorption. However, TG and total cholesterol (TC) levels were not remarkably changed in the $Klf9^{-/-}$ mice (Fig. 1c). We next examined the mRNA levels of genes involved in hepatic bile acid metabolism. The expression of hepatic Cyp7a1 and Cyp27a1 was substantially increased, as shown in Fig. 1d. Bsep mRNA levels increased by approximately twofold in the $Klf9^{-/-}$ mice. In comparison, the mRNA levels of Cyp8b1, *Shp*, *Fxr* and other transporters (Oatp, Mdr2, Ost-α and Ntcp) did not remarkably change (Fig. 1d). We also extracted intestinal RNAs from the WT and $Klf9^{-/-}$ mice. We found that mRNA levels of Fgf15, Asbt and Ost-α were decreased significantly (Fig. 1e), however, the mRNA levels of Fxr were not altered (Fig. 1e). Correspondingly, protein levels of Cyp7a1 in the liver, and Asbt and Fgf15 in the intestine were altered (Fig. 1f,g). Furthermore, we generated liver-specific Klf9-KO mice ($Klf9^{alb-/-}$) by crossing albumin-Cre with $Klf9^{flox/flox}$ mice to explore whether hepatic Klf9 deficiency contributes to the dysregulation of BA homeostasis. Real-time PCR data confirmed that hepatic Klf9 was efficiently deleted in the $Klf9^{alb-/-}$ mice (Fig. 2c, Supplementary Fig. 1a, b). However, we did not observe a change in the BA pool in the $Klf9^{alb-/-}$ mice (Fig. 2a, b). Moreover, the expression levels of genes involved in hepatic BA synthesis (Cyp7a1, Cyp8b1, Cyp27a1,Shp and Fxr) and BA transport (Oatp, Mdr2, Bsep, Ntcp and Ost-a) were not remarkably altered (Fig. 2c). In addition, the expression of genes involved in ileal BA metabolism, including Fgf15, Fxr,Asbt and Ostα, was not significantly influenced (Fig. 2d). The protein levels were consistent with the RNA levels (Fig. 2e, f). These findings suggest that the dysregulated bile acid metabolism in global Klf9-deficient mice can not be attributed to hepatic Klf9 deficiency.

Klf9 affects BA metabolism in the intestine

We next obtained intestinal epithelium-specific Klf9-KO mice ($Klf9^{vil-/-}$) by crossing villin-Cre^{+} with $Klf9^{flox/flox}$ mice to determine whether the change in BAs in the global Klf9 deficient mice was due to intestinal effects. Again, real-time PCR confirmed the efficient deletion of Klf9 in the intestine of the $Klf9^{vil-/-}$ mice (Fig. 3c, Supplementary Fig. 1c,d). As a result, the $Klf9^{vil-/-}$ mice exhibited an increase in gallbladder volume and BA levels in the gallbladder and faeces, while BA levels in the serum were decreased in the $Klf9^{vil-/-}$ mice compared with the $Klf9^{flox/flox}$ control mice (Fig. 3a, b). The mRNA levels of Fgf15 in the ileum were remarkably decreased in the $Klf9^{vil-/-}$ mice. The Asbt mRNA levels were lower by twofold in the $Klf9^{vil-/-}$ mice than in the control mice (Fig. 3c). In comparison, changes in the mRNA levels of Ostα and Fxr were not significant (Fig. 3c). We examined the expression levels of genes related to BA biosynthesis (Cyp7a1, Cyp8b1, Cyp27a1, Shp and Fxr), reuptake of BAs (Oatp, Ostα and Ntcp), and biliary excretion of BAs (Bsep and Mdr2) in the liver, as shown in Fig. 3d. We found that the mRNA levels of genes encoding BA biosynthetic enzymes (Cyp7a1, Cyp8b1 and Cyp27a1) and BA transporters (Mdr2 and Bsep) were remarkably increased in $Klf9^{vil-/-}$ mice (Fig. 3d), while the expression of Fxr, Shp, Oatp, Ostα and Ntcp showed little change (Fig. 3d). Cyp7a1 protein levels were remarkably increased in the $Klf9^{vil-/-}$ mice (Fig. 3e). Furthermore, Klf9 deficiency decreased Asbt and Fgf15 protein levels in the ileum (Fig. 3f). Thus, we concluded that Klf9 in the intestine regulates systemic BA homeostasis.

Klf9 induces Asbt expression in the terminal ileum

The above results suggest that Klf9 regulating bile acid metabolism involves Asbt and ileum-derived Fgf15. We infected primary small intestinal epithelial cells with an adenovirus overexpressing Klf9 (Ad-Klf9) or knocking down Klf9 expression (Ad-shKlf9) to determine whether Klf9 regulates Asbt and Fgf15. The mRNA levels of Asbt increased in the cells infected with Ad-Klf9 and were reduced in the Ad-shKlf9-infected cells (Fig. 4a, b). The mRNA levels of Fgf15 were not remarkably changed (Fig. 4a, b). Moreover, we obtained similar results in a human colon carcinoma cell line (Caco2) (Fig. 4c, d). Luciferase reporter gene assays revealed that Klf9 activates Asbt gene promoter activity but not the Fgf15 gene promoter (Fig. 3e, f). Chromatin immunoprecipitation (ChIP) analyses confirmed Klf9 protein occupancy at multiple consensus binding sites (CTGGC or G/C-rich elements) within the endogenous

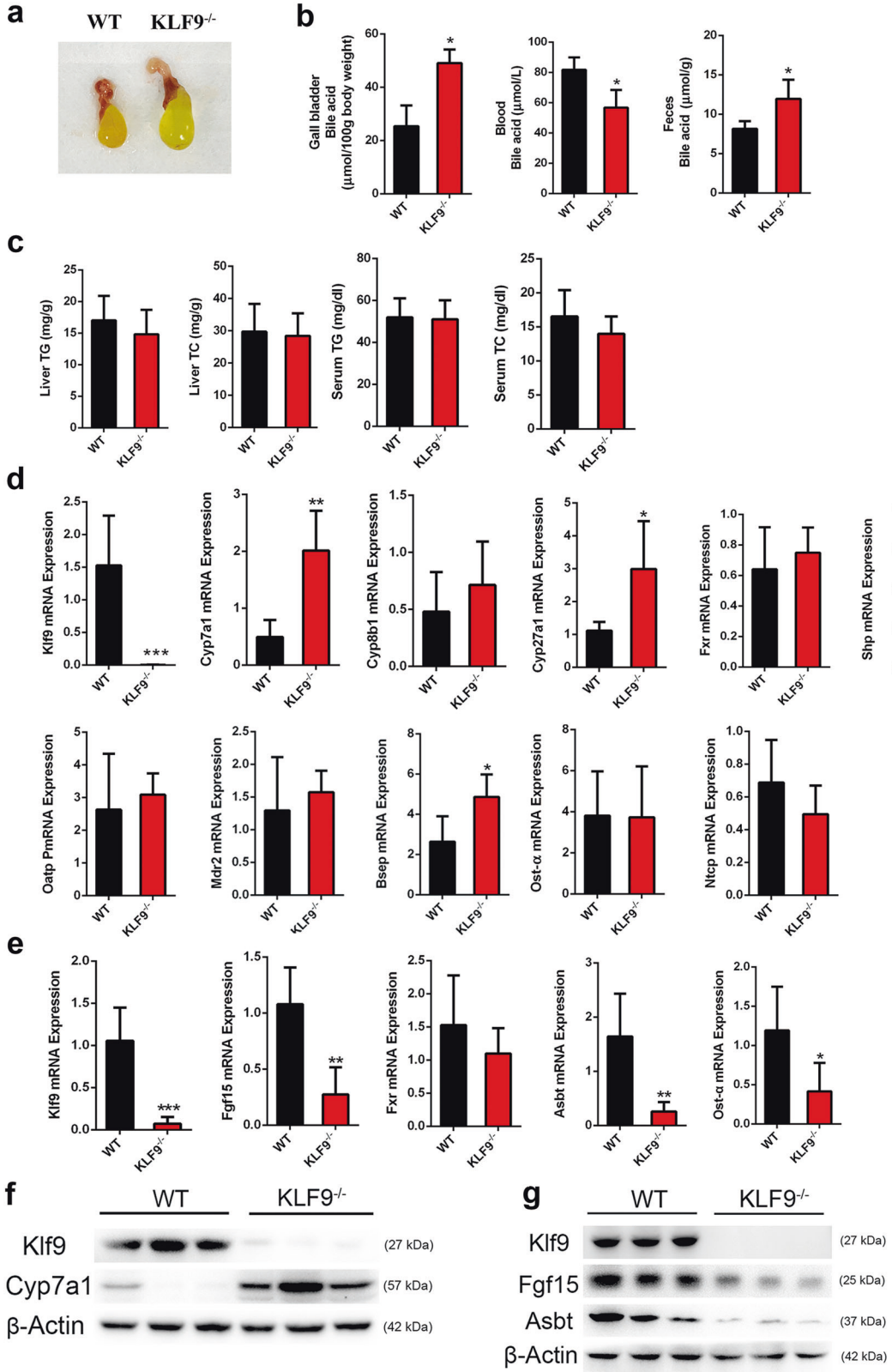

Fig. 1 Klf9 deletion results in BA dysregulation in enterohepatic circulation. a Images of gallbladders from the WT and Klf9$^{-/-}$ mice. **b** BA levels in the gallbladder, faeces and serum of the WT and Klf9$^{-/-}$ mice. **c** TG and TC levels in the livers and serum of the WT and Klf9$^{-/-}$ mice. **d** mRNA expression levels of Klf9, Cyp7a1, Cyp8b1, Cyp27a1, Shp, Fxr, Oatp, Mdr2, Bsep, Ntcp and Ostα in the livers of the WT and Klf9$^{-/-}$ mice. Gene expression was normalised to 36B4 expression. **e** mRNA expression levels of Klf9, Fgf15, Asbt, Fxr, and Ost-α in the intestines of the WT and Klf9$^{-/-}$ mice. Gene expression was normalised to 36B4 expression. **f** Protein expression levels of Klf9 and Cyp7a1 in the livers of the WT and Klf9$^{-/-}$ mice. β-actin served as the loading control. **g** Protein expression levels of Klf9, Asbt and Fgf15 in the intestines of the WT and Klf9$^{-/-}$ mice. β-actin served as the loading control. Data are represented as the mean ± SEM. *$P < 0.05$, **$P < 0.01$, ***$P < 0.001$ (**b**–**e**).

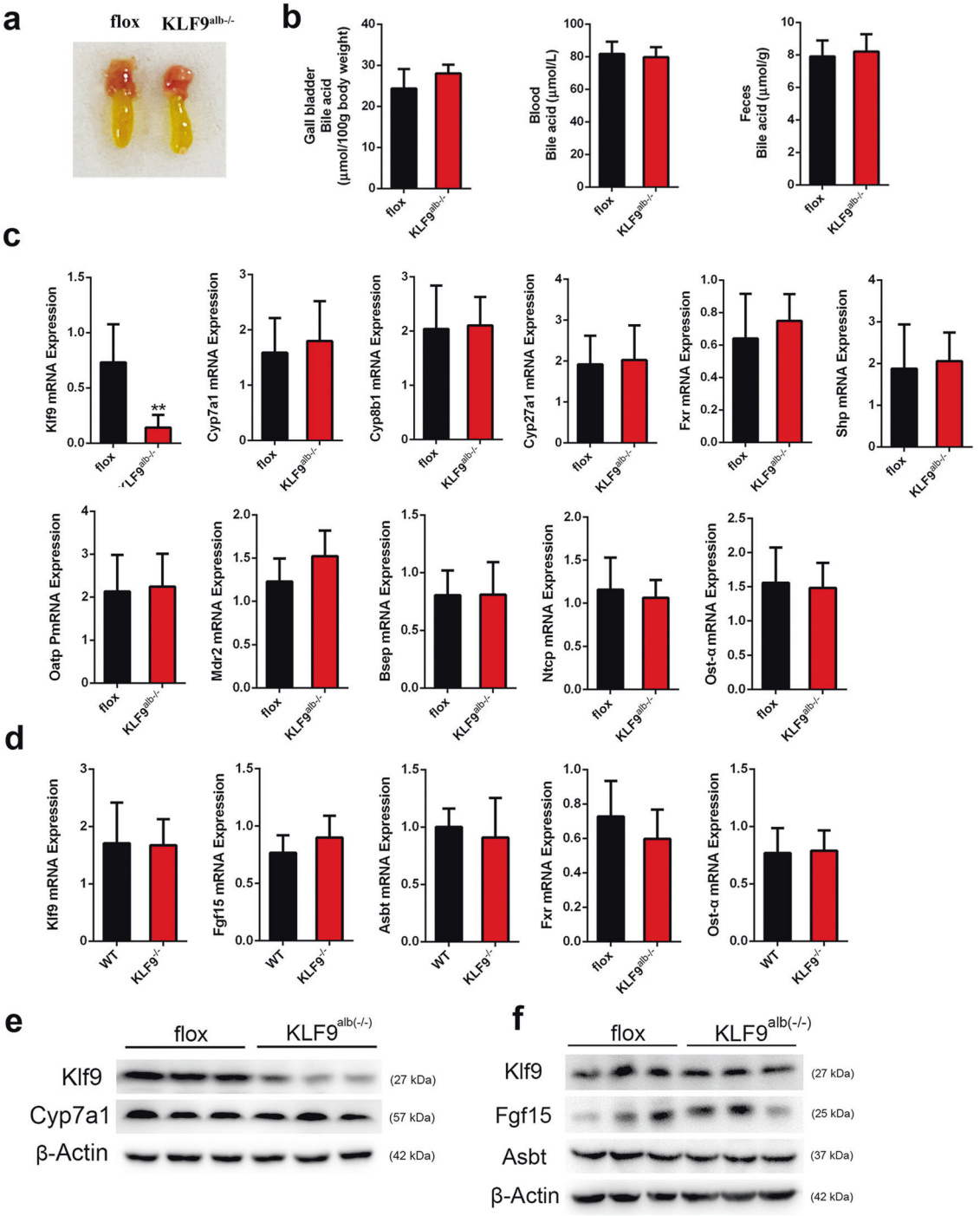

Fig. 2 Klf9 regulation of BA synthesis has a nonhepatic basis. a, **b** Images of gallbladder and BA levels in the gallbladder, faeces and serum of the control ($Klf9^{flox/flox}$) and liver-specific Klf9-KO ($Klf9^{alb-/-}$) mice. **c** mRNA expression levels of Klf9, Cyp7a1, Cyp8b1, Cyp27a1, Shp, Fxr, Oatp, Mdr2, Bsep, Ntcp and Ost-α in the livers of the $Klf9^{flox/flox}$ and $Klf9^{alb-/-}$ mice. Gene expression was normalised to 36B4 expression. **d** mRNA expression levels of Klf9, Fgf15, Asbt, Fxr, and Ost-α in the intestines of the $Klf9^{flox/flox}$ and $Klf9^{alb-/-}$ mice. Gene expression was normalised to 36B4 expression. **e** Protein expression levels of Klf9 and Cyp7a1 in the livers of the $Klf9^{flox/flox}$ and $Klf9^{alb-/-}$ mice. Actin served as the loading control. **f** Protein expression levels of Klf9, Asbt and Fgf15 in the intestines of the $Klf9^{flox/flox}$ and $Klf9^{alb-/-}$ mice. β-actin served as the loading control. Data are represented as the mean ± SEM. $^{**}P < 0.01$ (**b**–**d**).

Asbt promoter (Fig. 3g, h). Together, these results demonstrated that Asbt is the downstream target of the transcription factor Klf9.

BA absorption in Klf9 transgenic mice is increased

We next crossed Rosa26-Klf9 knock-in mice with Villin-cre mice to generate $Klf9^{Rosa26+/+}$ mice overexpressing Klf9 specifically in the intestinal epithelium to confirm the above results in vivo. The efficiency of Klf9 overexpression was verified at the mRNA level (Fig. 5c, Supplementary Fig. 1e,f). We examined the BA levels in the gallbladder, serum and faeces of the $Klf9^{Rosa26+/+}$ mice. The gallbladder volume was smaller than that in the controls (Fig. 5a). BA levels in the gallbladder and faeces were reduced whereas BA levels in the serum were increased in the $Klf9^{Rosa26+/+}$ mice compared with the corresponding control mice (Fig. 5b). As

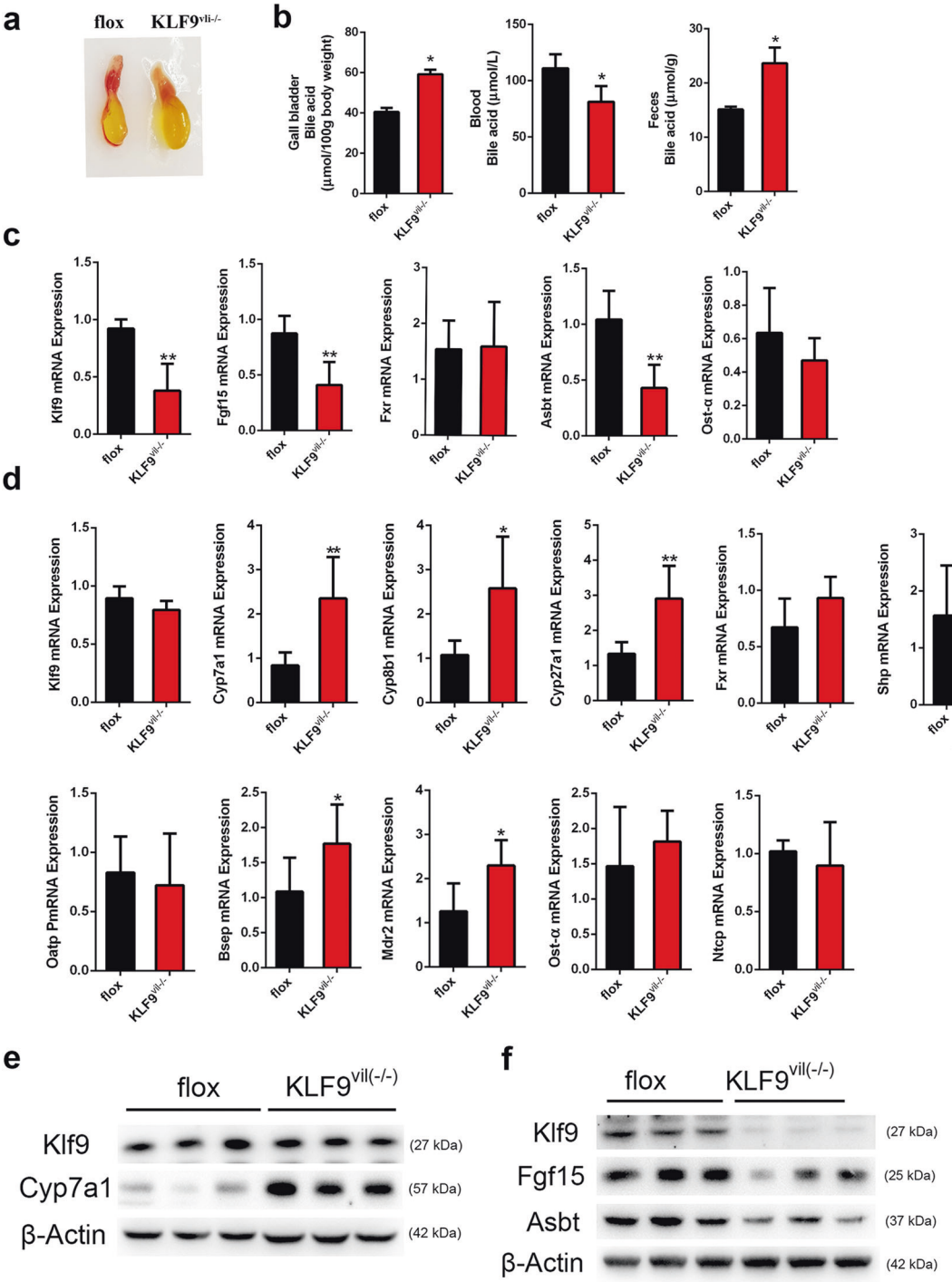

Fig. 3 Klf9 affects BA metabolism in the intestine. a Images of gallbladders in the control ($Klf9^{flox/flox}$) and intestine-specific Klf9-KO ($Klf9^{vil-/-}$) mice. **b** BA levels in the gallbladder, serum and faeces of the $Klf9^{flox/flox}$ and $Klf9^{vil-/-}$ mice. **c** mRNA expression levels of Klf9, Fgf15, Asbt, Fxr and Ost-α in the intestines of the $Klf9^{flox/flox}$ and $Klf9^{vil-/-}$ mice. Gene expression was normalised to 36B4 expression. **d** mRNA expression levels of Klf9, Cyp7a1, Cyp8b1, Cyp27a1, Shp, Fxr, Oatp, Mdr2, Bsep, Ntcp and Ostα in the liver tissues of the $Klf9^{flox/flox}$ and $Klf9^{vil-/-}$ mice. Gene expression was normalised to 36B4 expression. **e** Protein expression levels of Klf9 and Cyp7a1 in the intestines of the $Klf9^{flox/flox}$ and $Klf9^{vil-/-}$ mice. β-actin served as the loading control. **f** Protein expression levels of Klf9, Fgf15, and Asbt in the livers of the $Klf9^{flox/flox}$ and $Klf9^{vil-/-}$ mice. β-actin served as the loading control. Data are represented as the mean ± SEM. $^{*}P < 0.05$, $^{**}P < 0.01$ (**b**–**d**).

shown in Fig. 5c, the expression of Asbt and Fgf15 was remarkably higher in the ileum of the $Klf9^{Rosa26+/+}$ mice. Consistent with the enhanced intestinal BA reabsorption, the mRNA levels of hepatic genes associated with BA metabolism also changed considerably. The expression of genes related to bile acid synthesis (Cyp7a1 and Cyp27a1) and bile acid transporters (Mdr2) was remarkably reduced in the $Klf9^{Rosa26+/+}$ group (Fig. 4d). The expression of Oatp, which transports BAs from the portal blood into hepatocytes, was substantially increased (Fig. 4d), whereas the expression of other genes showed little change (Fig. 4d). The Cyp7a1 protein

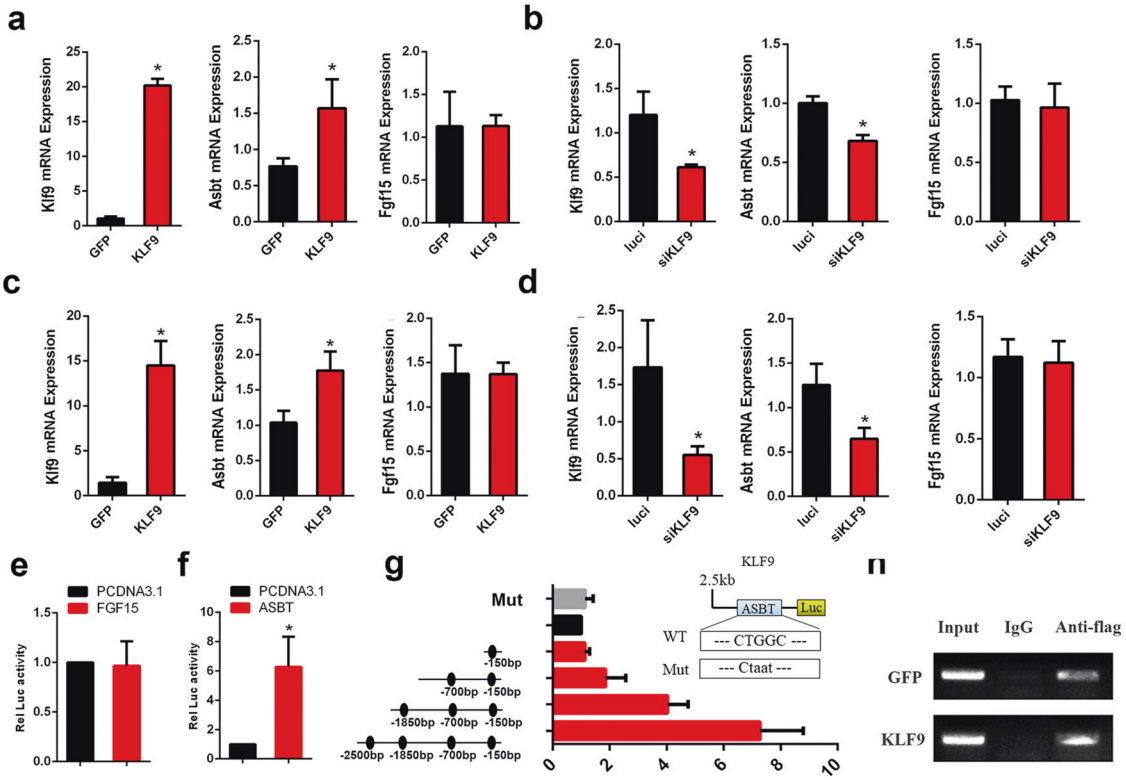

Fig. 4 Klf9 induces Asbt expression in the terminal ileum. Primary small intestinal epithelial cells (**a**, **b**) and Caco-2 cells (**c**, **d**) were infected with adenovirus with Klf9 overexpression (Klf9) or Klf9 KO (siKlf9). The mRNA expression levels of Klf9, Asbt, and Fgf15 were analysed by RT-qPCR. Gene expression was normalised to 36B4 expression. Dual-luciferase reporter gene assays of the (**e**) Fgf15 promoter (−2500 bp) and (**f**) ABST promoter (−2500 bp) were performed in HEK-293A cells. **g** The wild-type putative Klf9-binding element and its mutant sequence in the Asbt promoter region. A series of Asbt promoters fused to the luciferase reporter gene (−2500, −1850, −700, and −150 bp) were cotransfected into HEK-293A cells together with Klf9 expression plasmids or pc-DNA3.1 (control, Ctl). **h** ChIP assays were performed to confirm Klf9 binding to the Asbt gene promoter. Data are represented as the mean ± SEM. *$P < 0.05$ (**a**–**f**).

expression markedly decreased in the liver of the $Klf9^{Rosa26+/+}$ mice (Fig. 4e). The trends of Asbt and Fgf15 protein levels were similar to those of the mRNA levels (Fig. 4f). These changes suggest that Klf9 in the intestine contributes to the regulation of the BA pool level.

Morphology of the small intestine

No difference in body weight was observed among the four genotypes (Supplementary Fig. 2a). The mice showed no evidence of biochemical and histopathological changes in the liver (Supplementary Fig. 2b,c). No substantial changes in the intestine (jejunum, ileum and colon) were found among the four genotypes of mice (Fig. 6a). We measured serum Fgf15 protein levels by plasma enzyme-linked immunosorbent assays (ELISAs) of the mice with four genotypes and found that serum Fgf15 levels decreased in the $Klf9^{vil-/-}$ mice and increased in the $Klf9^{Rosa26+/+}$ mice (Fig. 6b). Immunohistochemical staining showed that Asbt protein levels were slightly lower in the $Klf9^{vil-/-}$ mice and higher in the $Klf9^{Rosa26+/+}$ mice than in the corresponding controls (Fig. 6c). The Asbt protein was identified in the epithelial cells of the villi (Fig. 6c). Immunofluorescence assays showed that the immunofluorescence intensity of Fgf15 was reduced in the $Klf9^{vil-/-}$ mice compared with the $Klf9^{flox/flox}$ control mice and enhanced in the intestinal epithelial cytoplasm of the $Klf9^{Rosa26+/+}$ mice compared with that of the Rosa26 (control) mice (Fig. 6d).

DISCUSSION

BA reabsorption in the intestine is a key step in BA metabolism; thus, alterations in BA transport could strongly influence the circulating homeostasis of BA metabolites [27–29]. In the present study, we show for the first time that Klf9 in the intestine mediates the enterohepatic recycling of BAs (Fig. 7).

As another member of the Klf transcription factor family, Klf15 has also been shown to regulate BA homeostasis. Liver-specific Klf15 deficiency results in the abnormal metabolism of BAs [30]. Klf15, as an endogenous regulator of Fgf15, controls circadian BA production [30]. In the present study, we found that Klf9 also affects the metabolism of BAs. The results showed that BA levels in the gallbladder and faeces increased and BA levels in the serum decreased in the systemic Klf9 KO mice. This phenomenon was not observed in the liver-specific Klf9 KO mouse model. However, a similar phenotype was obtained in the $Klf9^{vil-/-}$ mouse model. The results suggested that the regulation of BA metabolism by Klf9 may occur in the intestine. Fgf15 expression in vivo is related to Klf9 in the intestine. However, modulation of Klf9 expression by adenovirus did not significantly affect Fgf15 in primary intestinal epithelial cells or Caco-2 cells. Moreover, we observed that the mRNA and protein levels of Asbt markedly decreased in the intestines of the systemic Klf9 KO mice and the $Klf9^{vil-/-}$ mice. Previous studies indicated that Asbt repression resulted in lower plasma BA levels, more faecal BA loss and hepatic BA secretion [16, 31, 32]. Their results are consistent with our findings. We speculated that Asbt expression was disrupted in the in Klf9-KO mice, which resulted in BA metabolic disorder.

We observed that the direct binding of Klf9 to the Asbt promoter was mediated by GC-rich elements. The mRNA levels of Asbt increased in the cells infected with Ad-Klf9 and were reduced in the Ad-shKlf9 -infected cells. Previous studies have also shown that Asbt expression indeed undergoes negative feedback by BAs

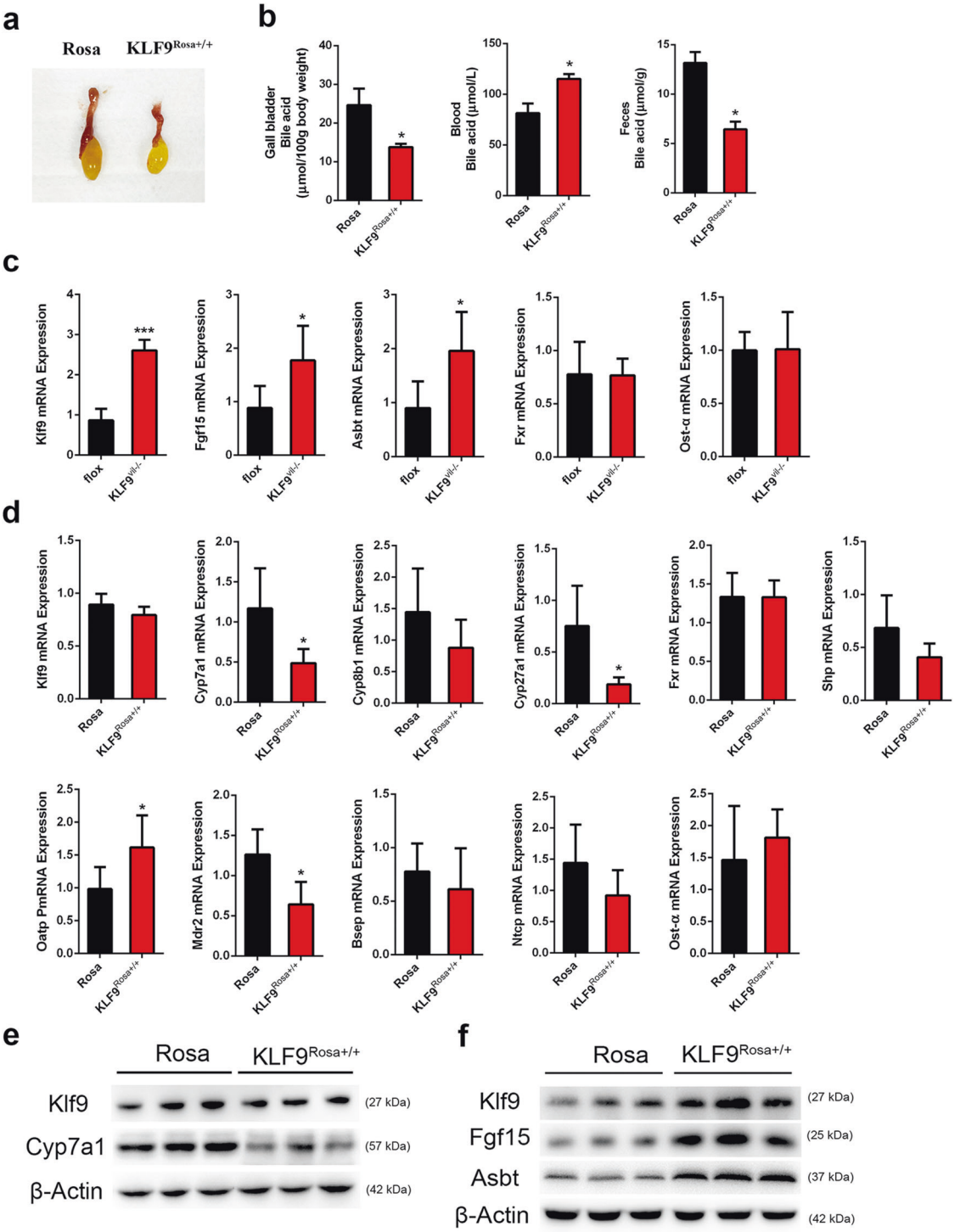

Fig. 5 Klf9 overexpression promotes BA reabsorption. a Images of gallbladders in the control (Rosa) and intestine-specific Klf9-overexpressing ($Klf9^{Rosa+/+}$) mice. **b** BA levels in the gallbladder, serum and faeces of the Rosa and $Klf9^{Rosa+/+}$ mice. **c** mRNA expression levels of Klf9, Fgf15, Asbt, Fxr and Ost-α in the intestines of the Rosa and $Klf9^{Rosa+/+}$ mice. Gene expression was normalised to 36B4 expression. **d** mRNA expression levels of Klf9, Cyp7a1, Cyp8b1, Cyp27a1, Shp, Fxr, Oatp, Mdr2, Bsep, Ntcp and Ost-α in the livers of the Rosa and $Klf9^{Rosa+/+}$ mice. **e** Protein expression levels of Klf9 and Cyp7a1 in the intestines of the Rosa and $Klf9^{Rosa+/+}$ mice. β-actin served as the loading control. **f** Protein expression levels of Klf9, Fgf15, and Asbt in the livers of the Rosa and $Klf9^{Rosa+/+}$ mice. β-actin served as the loading control. Data are represented as the mean ± SEM. $^{*}P < 0.05$, $^{***}P < 0.001$ (**b**–**d**).

and that altered Asbt expression could change BA signaling [33]. Fgf15 is a gut-derived hormone and a trigger of gallbladder emptying and refilling [34, 35]. Fgf15 is the hub of the gut–hepatic signal axis that regulates BA homeostasis [36]. The promotion of Asbt expression by Klf9 to affect BA homeostasis in vivo may be achieved through Fgf15 feedback. Fgf15, which is secreted by cells in the intestinal and bile duct epithelium, also plays an important role in the regulation of Asbt expression [37, 38]. Fgf15 signals from the intestine to the liver to repress Cyp7a1, which catalyses the first and rate-limiting step in the classic BA synthetic pathway

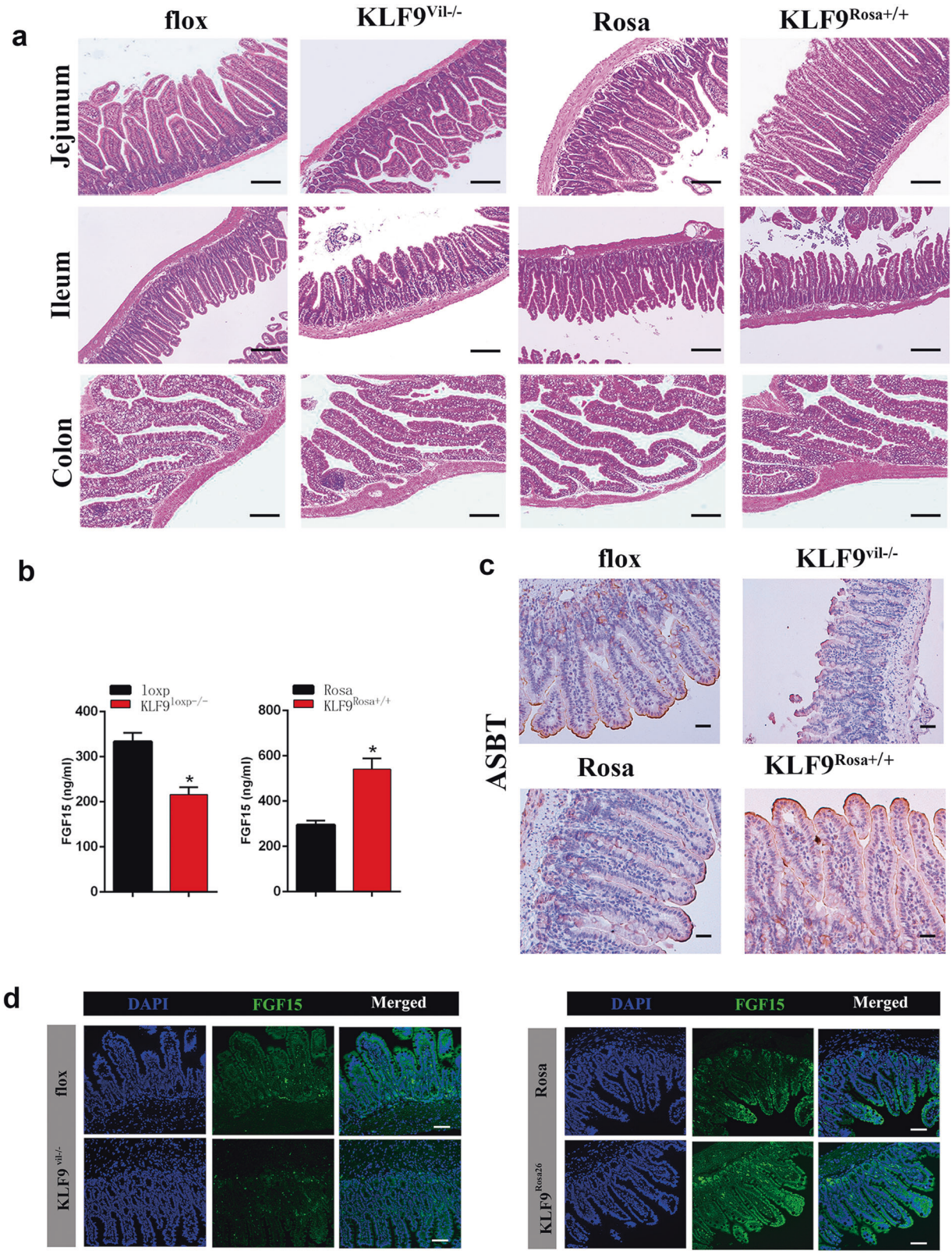

Fig. 6 Changes in small intestine morphology. a HE staining of the jejunum, ileum and colon in flox/flox mice, Klf9$^{vil-/-}$ mice, Rosa mice and Klf9$^{Rosa+/+}$ mice; images are shown at ×200 magnification; scale bars, 100 μm. **b** Fgf15 protein concentration in blood from the four groups. **c** Immunohistochemical staining of Asbt in the ileums of the four groups; images are shown at ×400 magnification; scale bars, 50 μm. **d** Representative immunofluorescence staining of Fgf15 in the intestinal tissues in the four groups; images are shown at ×400 magnification; scale bars, 50 μm. *$P < 0.05$.

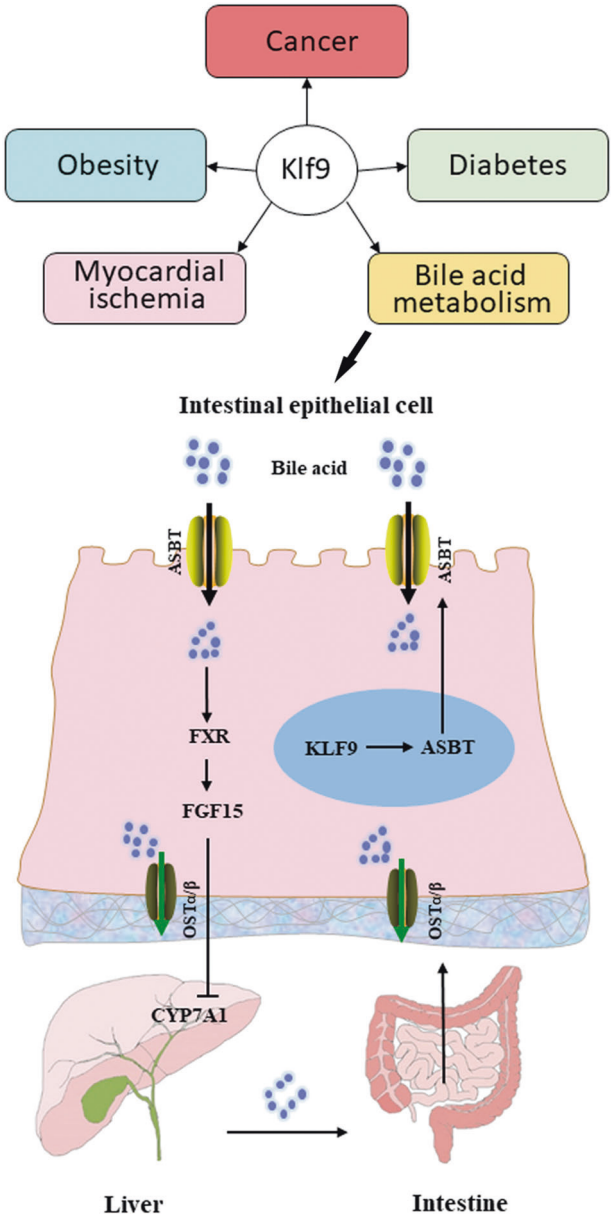

Fig. 7 Proposed model of Klf9 induction of BAs absorption. Proposed model of Klf9 induction of BA absorption. Klf9 promotes Asbt expression in the ileum, and Asbt promotes BA reabsorption. The reabsorbed BAs activate the Fxr/Fgf15 signalling pathway. Fgf15 is secreted from the intestine to repress Cyp7a1 expression in the liver and reduce BA production.

[12]. In the absence of Klf9, BA absorption by the small intestine was reduced, leading to inhibition of Fgf15 expression and the augmentation of BA synthetic enzymes in the liver. In summary, we identified for the first time that Klf9 is an upstream transcription factor of the Asbt gene and that Klf9/Asbt are components of the gut–liver signaling pathway that regulate BA synthesis.

A previous study showed that Klf9 in young mice (4 weeks old) controls crypt cell proliferation and differentiation within the intestine and colon [24]. In the present study, we did not observe the loss of crypt stem cells in the Klf9-deficient mice. We speculate that the difference is because adult mice (8–10 weeks old) were used in our experiment, and the dysplasia of the intestine was compensated for by other genes.

Together,our results demonstrated that Klf9 directly promotes Asbt expression in the ileum and reduces BA production in the liver through the Fgf15 signaling pathway.

ACKNOWLEDGEMENTS

This work was supported by the National Natural Science Foundation of China (grants 81730024 and 81825004), the National Key Research and Development Program of China (2018YFA0800601), the Scientific and Technological Research Project of Xinjiang Production and Construction Corps (grants 2018AB018 and 2021AB028) and the Tianjin Research Innovation Project for Postgraduate Students (2021YJSB259).

AUTHOR CONTRIBUTIONS

YSC, SL, and ML designed research studies. YLZ, YJZ and CYD contributed to the methodology. MLZ and CZW contributed to the investigation. SL, ML, MLZ, SFS, WW, YTF, JNS, JCH, YYF, WQ, JLH YHL provided formal analysis. YSC contributed to the validation. SL and ML wrote the original draft of the manuscript. LZ, JZ, YSC acquired funding.

ADDITIONAL INFORMATION

Supplementary information The online version contains supplementary material available at https://doi.org/10.1038/s41401-021-00850-x.

Competing interests: The authors declare no competing interests.

REFERENCES

1. Dawson PA, Lan T, Rao A. Bile acid transporters. J Lipid Res. 2009;50:2340–57.
2. Gonzalez FJ. Nuclear receptor control of enterohepatic circulation. Compr Physiol. 2012;2:2811–28.
3. Chiang JY. Regulation of bile acid synthesis: pathways, nuclear receptors, and mechanisms. J Hepatol. 2004;40:539–51.
4. de Aguiar Vallim TQ, Tarling EJ, Edwards PA. Pleiotropic roles of bile acids in metabolism. Cell Metab. 2013;17:657–69.
5. Li T, Matozel M, Boehme S, Kong B, Nilsson LM, Guo G, et al. Overexpression of cholesterol 7alpha-hydroxylase promotes hepatic bile acid synthesis and secretion and maintains cholesterol homeostasis. Hepatology. 2011;53:996–1006.
6. Galman C, Angelin B, Rudling M. Pronounced variation in bile acid synthesis in humans is related to gender, hypertriglyceridaemia and circulating levels of fibroblast growth factor 19. J Intern Med. 2011;270:580–8.
7. Zhu Y, Liu H, Zhang M, Guo GL. Fatty liver diseases, bile acids, and FXR. Acta Pharm Sin B. 2016;6:409–12.
8. Kouzuki H, Suzuki H, Ito K, Ohashi R, Sugiyama Y. Contribution of sodium taurocholate co-transporting polypeptide to the uptake of its possible substrates into rat hepatocytes. J Pharmacol Exp Ther. 1998;286:1043–50.
9. Boyer JL, Trauner M, Mennone A, Soroka CJ, Cai SY, Moustafa T, et al. Upregulation of a basolateral FXR-dependent bile acid efflux transporter OSTalpha-OSTbeta in cholestasis in humans and rodents. Am J Physiol Gastrointest Liver Physiol. 2006;290:G1124–1130.
10. Stieger B, Meier Y, Meier PJ. The bile salt export pump. Pflug Arch. 2007;453:611–20.
11. Goodwin B, Jones SA, Price RR, Watson MA, McKee DD, Moore LB, et al. A regulatory cascade of the nuclear receptors FXR, SHP-1, and LRH-1 represses bile acid biosynthesis. Mol Cell. 2000;6:517–26.
12. Inagaki T, Choi M, Moschetta A, Peng L, Cummins CL, McDonald JG, et al. Fibroblast growth factor 15 functions as an enterohepatic signal to regulate bile acid homeostasis. Cell Metab. 2005;2:217–25.
13. Wong MH, Oelkers P, Craddock AL, Dawson PA. Expression cloning and characterization of the hamster ileal sodium-dependent bile acid transporter. J Biol Chem. 1994;269:1340–7.
14. Craddock AL, Love MW, Daniel RW, Kirby LC, Walters HC, Wong MH, et al. Expression and transport properties of the human ileal and renal sodium-dependent bile acid transporter. Am J Physiol. 1998;274:G157–169.
15. Degirolamo C, Rainaldi S, Bovenga F, Murzilli S, Moschetta A. Microbiota modification with probiotics induces hepatic bile acid synthesis via downregulation of the Fxr-Fgf15 axis in mice. Cell Rep. 2014;7:12–18.
16. Rao A, Kosters A, Mells JE, Zhang W, Setchell KD, Amanso AM, et al. Inhibition of ileal bile acid uptake protects against nonalcoholic fatty liver disease in high-fat diet-fed mice. Sci Transl Med. 2016;8:357ra122.

17. Cicione C, Degirolamo C, Moschetta A. Emerging role of fibroblast growth factors 15/19 and 21 as metabolic integrators in the liver. Hepatology. 2012;56:2404–11.
18. Byun S, Kim DH, Ryerson D, Kim YC, Sun H, Kong B, et al. Postprandial FGF19-induced phosphorylation by Src is critical for FXR function in bile acid homeostasis. Nat Commun. 2018;9:2590.
19. Sogawa K, Imataka H, Yamasaki Y, Kusume H, Abe H, Fujii-Kuriyama Y. cDNA cloning and transcriptional properties of a novel GC box-binding protein, BTEB2. Nucleic Acids Res. 1993;21:1527–32.
20. Fan H, Zhang Y, Zhang J, Yao Q, Song Y, Shen Q, et al. Cold-inducible Klf9 regulates thermogenesis of brown and beige fat. Diabetes. 2020;69:2603–18.
21. Zhang Y, Xue Y, Cao C, Huang J, Hong Q, Hai T, et al. Thyroid hormone regulates hematopoiesis via the TR-KLF9 axis. Blood. 2017;130:2161–70.
22. Kasai S, Shimizu S, Tatara Y, Mimura J, Itoh K. Regulation of Nrf2 by mitochondrial reactive oxygen species in physiology and pathology. Biomolecules. 2020;10:320.
23. Otsuka K, Takehara A, Chiba N, Matsui Y. Identification of KLF9 and BCL3 as transcription factors that enhance reprogramming of primordial germ cells. PLoS One. 2018;13:e0205004.
24. Simmen FA, Xiao R, Velarde MC, Nicholson RD, Bowman MT, Fujii-Kuriyama Y, et al. Dysregulation of intestinal crypt cell proliferation and villus cell migration in mice lacking Kruppel-like factor 9. Am J Physiol Gastrointest Liver Physiol. 2007;292:G1757–1769.
25. Luo J, Deng ZL, Luo X, Tang N, Song WX, Chen J, et al. A protocol for rapid generation of recombinant adenoviruses using the AdEasy system. Nat Protoc. 2007;2:1236–47.
26. Cui A, Fan H, Zhang Y, Zhang Y, Niu D, Liu S, et al. Dexamethasone-induced Kruppel-like factor 9 expression promotes hepatic gluconeogenesis and hyperglycemia. J Clin Invest. 2019;129:2266–78.
27. Boesjes M, Brufau G. Metabolic effects of bile acids in the gut in health and disease. Curr Med Chem. 2014;21:2822–9.
28. Song X, Sun X, Oh SF, Wu M, Zhang Y, Zheng W, et al. Microbial bile acid metabolites modulate gut RORgamma^{+} regulatory T cell homeostasis. Nature. 2020;577:410–5.
29. Sinha SR, Haileselassie Y, Nguyen LP, Tropini C, Wang M, Becker LS, et al. Dysbiosis-induced secondary bile acid deficiency promotes intestinal inflammation. Cell Host Microbe. 2020;27:659–70. e655
30. Han S, Ray JW, Pathak P, Sweet DR, Zhang R, Gao H, et al. KLF15 regulates endobiotic and xenobiotic metabolism. Nat Metab. 2019;1:422–30.
31. Ovadia C, Perdones-Montero A, Spagou K, Smith A, Sarafian MH, Gomez-Romero M, et al. Enhanced microbial bile acid deconjugation and impaired ileal uptake in pregnancy repress intestinal regulation of bile acid synthesis. Hepatology. 2019;70:276–93.
32. Malhotra U, Concannon P. Human T-cell receptor CD3-delta (CD3D)/MspI DNA polymorphism. Nucleic Acids Res. 1989;17:2373.
33. Dawson PA. Roles of Ileal ASBT and OSTalpha-OSTbeta in regulating bile acid signaling. Dig Dis. 2017;35:261–6.
34. Uriarte I, Latasa MU, Carotti S, Fernandez-Barrena MG, Garcia-Irigoyen O, Elizalde M, et al. Ileal FGF15 contributes to fibrosis-associated hepatocellular carcinoma development. Int J Cancer. 2015;136:2469–75.
35. Zhou M, Luo J, Chen M, Yang H, Learned RM, DePaoli AM, et al. Mouse species-specific control of hepatocarcinogenesis and metabolism by FGF19/FGF15. J Hepatol. 2017;66:1182–92.
36. Wang Y, Gunewardena S, Li F, Matye DJ, Chen C, Chao X, et al. An FGF15/19-TFEB regulatory loop controls hepatic cholesterol and bile acid homeostasis. Nat Commun. 2020;11:3612.
37. Ghosh A, Chen F, Banerjee S, Xu M, Shneider BL. c-Fos mediates repression of the apical sodium-dependent bile acid transporter by fibroblast growth factor-19 in mice. Am J Physiol Gastrointest Liver Physiol. 2014;306:G163–171.
38. Neimark E, Chen F, Li X, Magid MS, Alasio TM, Frankenberg T, et al. c-Fos is a critical mediator of inflammatory-mediated repression of the apical sodium-dependent bile acid transporter. Gastroenterology. 2006;131:554–67.